WARSAW UNIVERSITY OF TECHNOLOGY Index 351733
FACULTY OF CIVIL ENGINEERING
COMMITTEE FOR CIVIL AND WATER ENGINEERING
POLISH ACADEMY OF SCIENCES ISSN 1230-2945

DOI: 10.24425/ace.2021.138048

ARCHIVES OF CIVIL ENGINEERING

Vol. LXVII ISSUE 3 2021

s. 139–155

Research paper

Load bearing capacity of laminated veneer lumber beams strengthened with CFRP strips

M. Bakalarz[1]

Abstract: The paper presents the results of experimental tests on the reinforcement of bent laminated veneer lumber beams with carbon fibre reinforced polymer (CFRP) strips glued to the bottom of elements. CFRP strips (1.4×43×2800 mm) were glued to the beams by means of epoxy resin. The tests were performed on full-size components with nominal dimensions of 45×200×3400 mm. Static bending tests were performed in a static scheme of the so-called four-point bending. The increase in the load bearing capacity of the reinforced elements (maximum bending moment and loading force) was 38% when compared to reference beams. A similar increase was noted in relation to the deflection of the elements at maximum loading force. For the global stiffness coefficient in bending, the increase for reinforced beams was 21%. There was a change in the way elements were destroyed from brittle, sudden destruction for reference beams resulting from the exhaustion of tensile strength to more ductile destruction initiated in the compressive zone for reinforced beams. The presented method can be applied to existing structures.

Keywords: 4-point bending, carbon fibre, reinforcement, timber structures

[1] MSc., Eng., Kielce University of Technology, Faculty of Civil Engineering and Architecture, Al. Tysiąclecia Państwa Polskiego 7, 25-314 Kielce, Poland, e-mail: mbakalarz@tu.kielce.pl, ORCID: https://orcid.org/0000-0003-1906-2175

1. Introduction

Mechanical properties of the wood depend on the direction of analysis relative to the axis of the tree trunk (anisotropy), location of the point of interest (heterogeneity) and several factors such as moisture content, density, wood temperature, service life, mechanical load [18]. Numerical analysis of the influence of anisotropy on the energy release rate for pinewood are presented in paper [28]. Analysis of the process of wood plasticization, considering different values of moisture content and temperature, are presented in paper [24].

Increasing the load bearing strength and stiffness of bent wooden structural elements is usually done by introducing reinforcement into an old [2, 19, 34] or new element. This reinforcement usually takes the form of rods [9], sheets (uni-, bi- or multi-directional reinforced) [10, 16, 17, 27, 36, 38], laminates [13] or profiles obtained by pultrusion [23, 39]. The conventional material from which these elements were made was steel [1,15] or other metals such as aluminium. Composite materials – aramid, glass, carbon or basalt fibres responsible for carrying the load immersed in the resin matrix have now become a popular solution [6, 26]. Fiber-reinforced polymer materials are characterized by lightweight and high mechanical properties. The connection between the reinforcement and the reinforced element is usually done by means of an epoxy resin adhesive or mechanical connectors.

Numerous papers, published since the 1960s [7], have been devoted to passive reinforcement of solid or laminated wood elements [8, 25]. The starting point of these considerations was the reinforcement scheme involving an application of reinforcement in the tensile zone, which is the response to a standard method of destruction resulting from a brittle fracture of an element. Modification of this scheme, enforced by the pursuit of effectiveness improvement, involves the addition of reinforcement inserts in the compressed part of a cross-section [12]. Reinforcement can be applied over the entire length of an element or on its parts [4]. When considering the position of the reinforcement in relation to a cross-section of a wooden element we can distinguish between [3, 14, 37]: inner reinforcement and outer reinforcement.

In order to increase the strengthening effectiveness, the reinforcement is prestressed, the so-called active reinforcement. The prestressing generates the precamber of the reinforced element and increases the utilization of the strength of the applied reinforcement. Among the prestressing effects, the authors [11, 35] also mention a significant increase in stiffness in addition to significant increases in load bearing capacity. An unusual solution was presented in the paper [5], where

compressed wood in the form of a block introduced in the compresive zone was used to prestress the elements.

The results of the tests are presented in this article as a continuation of the work on reinforcement of laminated veneer lumber beams. The papers [20, 21] discuss the reinforcement of LVL beams, on a laboratory scale, using composite sheets reinforced with aramid, glass and carbon fibres. Reinforcement of full-size beams with CFRP strips glued into the hollowed-out slots along the bottom surface is discussed in the publication [22]. The objective of this study is to evaluate strengthening effectiveness of LVL beams reinforced with CFRP laminates glued to the bottom face. A comparison of the internal and external type of reinforcement is described in the summary.

2. Materials and methods

2.1. Materials

2.1.1. Laminated veneer lumber

The full-size beams made of laminated veneer lumber (LVL) were used in research. The beams with dimensions of 45×200×3400 mm were tested in the edge-wise conditions. Selected properties of laminated veneer lumber are shown in Table 1. Control testing of the reinforced material is presented below to estimate the compressive strength parallel to the grain.

Table 1. Selected properties of laminated veneer lumber (exposed by manufacturer)

Parameter	Value
Bending strength [N/mm^2]	44
Tensile strength [N/mm^2]	36
Compressive strength parallel to grain [N/mm^2]	40
Modulus of elasticity [kN/mm^2]	14
Shear modulus [N/mm^2]	600

The compressive strength parallel to grain was estimated on samples cut from full-size beams on the Zwick 250 testing machine according to the guidelines of the standards [29, 31]. The geometric dimensions of the samples were selected taking into account the maximum possible load and

spacing of the testing machine heads. Nominal dimensions of the samples were 45×50×300 mm. The sample was placed between the articulated heads and their initial position was adjusted to the height of the test piece (the average preload was approximately 60 N). The load was applied at a constant speed of 0.01 mm/sec. The test results are presented in Table 2. Comparing with the data presented in Table 1, a higher compressive strength value and a higher dry density value were obtained.

a)  b) 

Fig. 1. Compressive strength parallel to grain test of LVL: a) specimen placed in testing machine, b) failure mode

Table 2. Compressive strength parallel to grain test results of LVL

Parameter	x [j]	s [j]	Vs [%]	R [j]
Maximum loading force [kN]	128.33	9.73	7.58	35.59
Compressive strength along the fibres [N/mm2]	58.55	4.98	8.50	17.72
Density [kg/m3]	598.41	21.30	3.56	62.93

Symbols: x – arithmetic mean, s – standard deviation, Vs – coefficient of variation, R – range, difference between maximum and minimum value, j – unit of analysed parameter

2.1.1. CFRP laminates

Unidirectional carbon fibre reinforced polymer strips were used to reinforce the LVL beams. The 1.4-mm-thick CFRP strip, supplied in rolls, was cut into 280-cm-long strips and the base width of the strip (50 mm) was reduced to 43 mm. The strip width was adjusted to the reinforced beam

width, taking into account the possible curvature of the elements. After cutting the reinforcement, its width was checked at three points – in the middle of the span and 15 cm from the beginning and end.

Material tests of CFRP strips were conducted on the Zwick 250 testing machine on 1.4×15×250 mm samples according to the guidelines contained in the standards [32, 33]. In order to prevent damage caused by samples breaking out of the testing machine jaws, 2×15×50 mm aluminium washers were glued to the ends of the samples with an epoxy adhesive. The distance between the washers was 150 mm. The load was applied at a constant feed speed of the testing machine heads of 2 mm/min. The test results are presented in Table 3.

a) 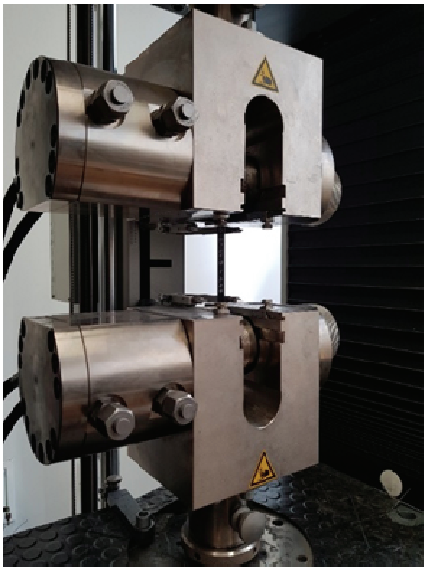 b) 

Fig. 2. Tensile strength tests of CFRP strips: a) specimen placed in testing machine, b) typical failure mode

Table 3. Tensile strength test results of CFRP strips

Parameter	x [j]	s [j]	Vs [%]	R [j]
Width [mm]	15.01	0.16	1.08	0.58
Maximum loading force [kN]	47.87	2.53	5.29	8.23
Tensile strength [N/mm^2]	2262.23	115.32	5.10	402.41
Modulus of elasticity [kN/mm^2]	198.90	6.19	3.11	22.00

Symbols: x – arithmetic mean, s – standard deviation, Vs – coefficient of variation, R – range, difference between maximum and minimum value, j – unit of analysed parameter

The CFRP strips were glued to the beams with a two-component epoxy adhesive. Before the adhesive application, the surface of the CFRP strip had been degreased. The surface of LVL beams, along the length of the reinforcement application, was ground and cleaned. The adhesive joint thickness was approximately 3 mm. The selected adhesive parameters are shown in Table 4.

Table 4. Selected mechanical and physical properties of epoxy resin (exposed by manufacturer)

Parameter	Value
Modulus of elasticity [N/mm^2]	7100
Density [g/cm^3]	1.7–1.8
Tensile strength [N/mm^2]	3
Compressive strength [N/mm^2]	70

2.2. Methods

The tests were conducted in the Material Strength Laboratory of the Kielce University of Technology. The tests were performed according to the guidelines contained in the standards [29, 31]. The subject of the tests was laminated veneer lumber beams reinforced with carbon strips glued to the bottom surface of the beams. The aim of the tests was to determine the impact of the reinforcement on the work of elements subjected to four-point bending test (load bearing capacity).

A view of the test bench is shown in Fig. 3. The reinforcement scheme for F beams is shown in Fig. 4. The total length of each beam was 340 cm. The span in the support axes was 15 times the height of the tested cross-section (300 cm).

The beams were loaded symmetrically with two concentrated forces, as shown in Fig. 3. The distance between the concentrated force axis and the axis of nearest support was 90 cm. The distance between the concentrated forces was 6 times the height of the cross section – 120 cm. The load was controlled by means of the sliding speed of the load thrust. The initial load of the tested components was 0.3kN in each actuator. The sliding speed of the load thrust was chosen experimentally so that the destruction of unreinforced elements takes place within the time interval of 180 to 420 seconds recommended by the standard [31]. In this way, the first element was tested at a sliding speed of thrust equal to (beam A1) 13 mm/min and the other elements at a speed equal to 7 mm/min.

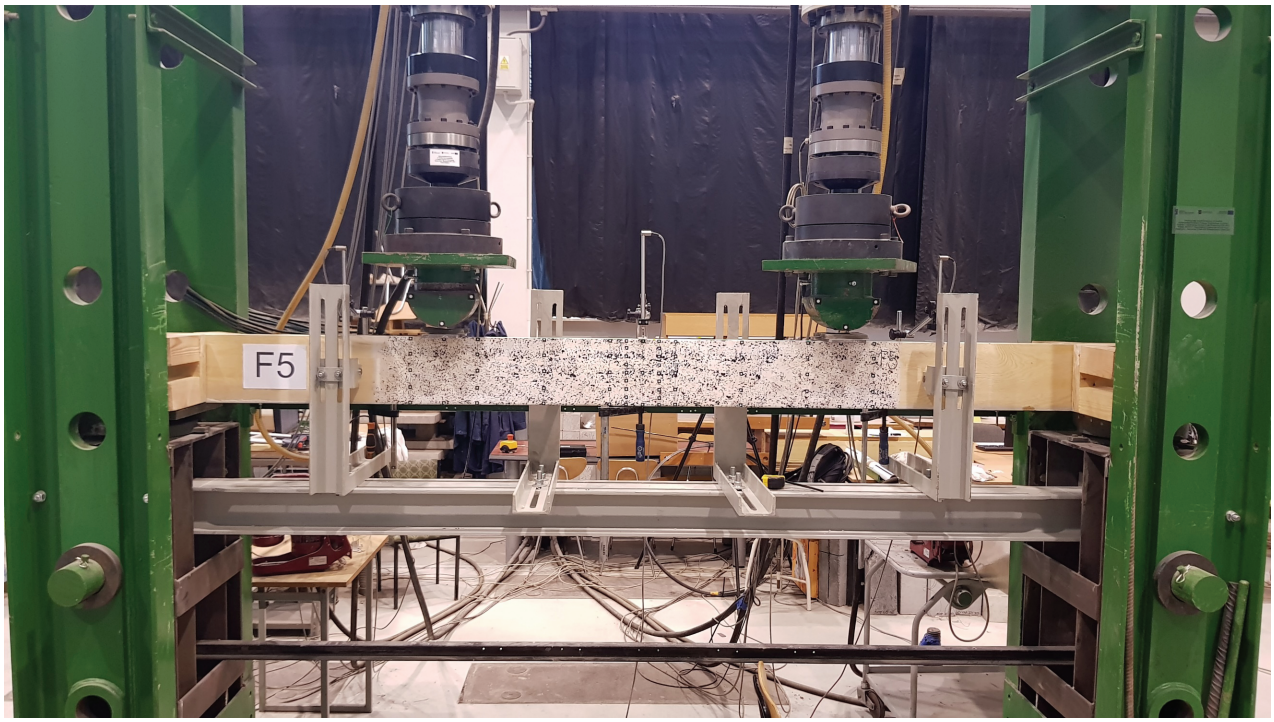

Fig. 3. The test bench setup

Steel plates were used, to prevent local indentation and to spread the load over a larger area, on supports and at the point of application of concentrated forces. The plates width was assumed to be half the height of the unreinforced cross section. The dimensions of steel plates were: 10 cm (width), 1 cm (thickness) and 20 cm (length).

Due to the testing of relatively slender elements, the test bench was equipped with additional protection against displacement of elements from the bending plane in the form of side supports (guides). Each side support had of a roller, on which the side surface of the beam moved during the test, placed on a support frame made of channel sections. The support frame allowed adjusting the height of the guide and its distance from the side surface of the elements. At the beginning of the test, the roller was applied at half of the unreinforced section height. The asymmetrical arrangement of the protections was forced by the dimensions of the load thrust heads and the need to expose the central part of the beam at the front in order to measure the deflections and deformations using an ARAMIS optical system. The distance between the axis of side supports and the nearest concentrated force axis was approximately 300 mm. In addition, wooden protections based on the test bench design construction were placed on the supports (P1, P2).

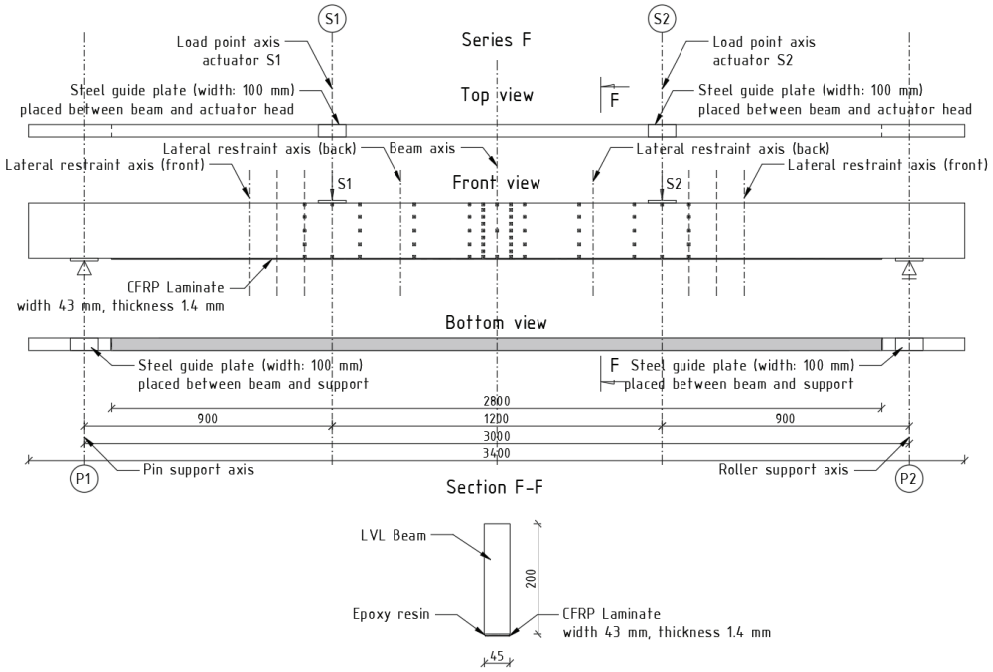

Fig. 4. The reinforcement scheme for F series

During the tests with the computer set, the following were recorded continuously (with a recording frequency of 5 Hz): load value in each actuator (S1, S2), test duration (T), deflection of the element in the middle of the span in the horizontal extremity of the compressed fibres (u). Based on these measurements, the following were estimated: total load (F), bending moments (M1, M2) at the points of application of concentrated forces and the bending moment (Mav) in the middle of the element span. After the tests, the way of destroying the elements was described and documented, and the humidity of the elements was checked with an electric resistance hygrometer.

3. Results

3.1. Load bearing capacity

The graph of the total load relation to the corresponding deflection measured with an inductive sensor at the centre of the beam span is shown in Fig. 5. The graph shows the average value of maximum load for unreinforced beams and indicates the element deflection limits for SLS [30]. There was an error in recording the deflection measurement at the beginning of the test for A1 and A5 beams. For the A beams, from the test start until the maximum force is reached, the curves describe the linear relationship between these parameters. Flattening of curves can be observed in the final testing stage for reinforced beams. This phenomenon is most evident for the F4 beam. This

can be identified by the greater use of the properties of the compressive zone and the increase in ductility during bending.

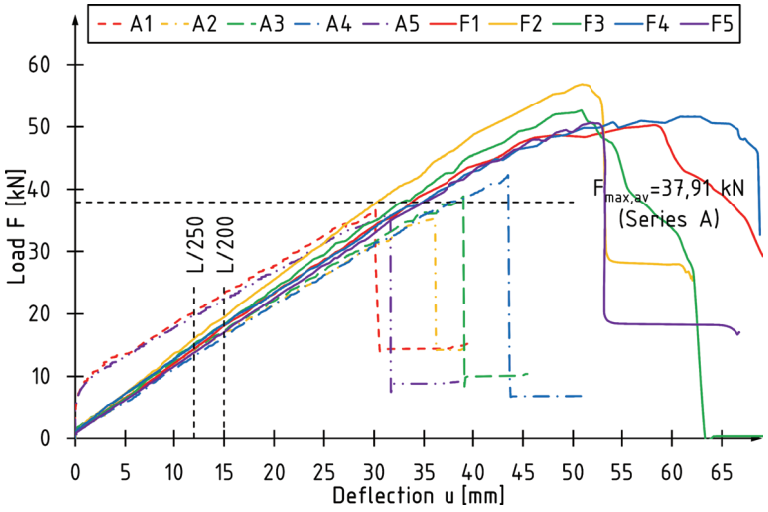

Fig. 5. The load-deflection diagram

The graph of the relationship between the total load and the test duration is shown in Fig. 6. As in the case of Fig. 5, the value of the average maximum force for the reference beams is marked with a horizontal line. In addition, vertical lines mark the limits of the range in which the destruction of unreinforced elements, tested according to the recommendations of the standard [31], and the middle of this range, were marked. Most of the unreinforced elements were destroyed within the recommended time frame. The exception is element A1, the destruction of which followed at the lower time frame limit. In the case of reinforced beams, the test duration was extended and some of the elements were outside the upper limit of the range.

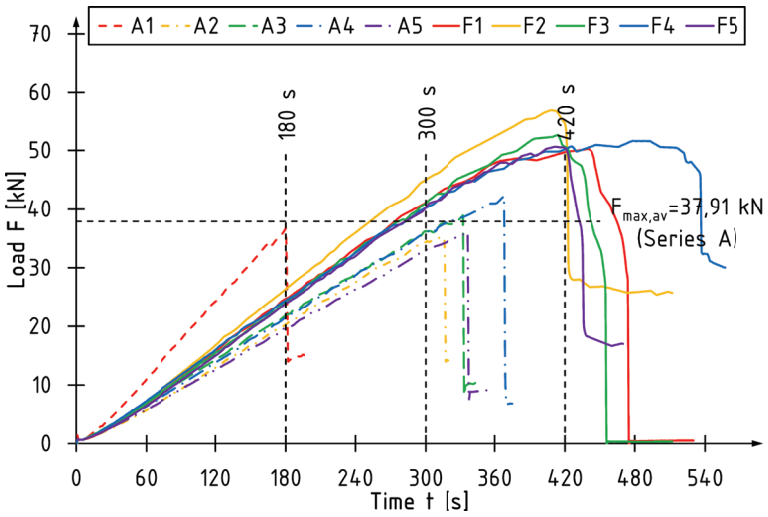

Fig. 6. The load-time diagram

Table 5 shows the detailed test results for the tested elements in relation to the maximum total load and the accompanying values for the other parameters to be recorded or determined, including: $S1_{Fmax}$ – force recorded in S1 actuator, in kilonewtons; $S2_{Fmax}$ – force recorded in S1 actuator, in kilonewtons; F_{max} – maximum loading force of the element (sum of S1 and S2) , in kilonewtons; uFmax - deflection when maximum loading is reached, in millimetres; T_{Fmax} – time at reaching the maximum load, in seconds; $M1_{Fmax}$ – bending moment at the point of application of the concentrated force S1, in kilonewton-metres; $M2_{Fmax}$ – bending moment at the point of application of the concentrated force S2, in kilonewton-metres; M_{avFmax} – value of the bending moment at the centre of the element span, in kilonewton-metres. The table also shows the value of the global modulus of elasticity (MOE) in bending determined according to the formula [31]:

$$E_{m,g} = \frac{3al^2 - 4a^3}{2bh^3\left(2\frac{w_2 - w_1}{F_2 - F_1} - \frac{6a}{5Gbh}\right)} \tag{1.1}$$

where:
$F_2 - F_1$ – load increment in elastic range [N], $w_2 - w_1$ – deflection increment corresponding to the load increment [mm], *b, h* – cross-section dimensions [mm], *a, l* – dimensions related to the static scheme [mm], *G* – shear modulus [N/mm^2].

Table 5. The results of experimental tests for ultimate limit state

Nr	$S1_{Fmax}$ [kN]	$S2_{Fmax}$ [kN]	F_{max} [kN]	u_{Fmax} [mm]	T_{Fmax} [s]	$M1_{Fmax}$ [kN]	$M2_{Fmax}$ [kN]	M_{avFmax} [kN]	MOE [GPa]
A1	16.41	20.46	36.87[1]	–	179.8	15.86[1]	17.32[1]	16.59	12.73[1]
A2	16.09	19.24	35.33[1]	36.06	314.8	15.33[1]	16.46[1]	15.90	14.50[1]
A3	18.90	20.00	38.89[1]	39.10	332.4	17.30[1]	17.70[1]	17.50	14.68[1]
A4	20.21	22.14	42.36[1]	43.56	367.6	18.71[1]	19.41[1]	19.06	15.09[1]
A5	16.11	19.97	36.08[1]	–	337.4	15.54[1]	16.93[1]	16.24	13.77[1]
F1	23.61	26.66	50.27	58.38	440.2	22.07	23.17	22.62	15.15
F2	27.10	29.76	56.86	50.90	408.4	25.11	26.07	25.59	16.37
F3	24.66	27.98	52.64	50.84	414.0	23.09	24.28	23.69	16.18
F4	22.19	29.42	51.61	60.82	477.8	21.92	24.53	23.23	15.20
F5	26.64	24.02	50.66	51.91	412.2	23.27	22.33	22.80	15.65

[1] Values published in work [22]

The average increase in total beam loading force and bending moment at the centre of the span was 38% (Table 6). The same increment was recorded for deflection. Locally – slightly lower values of recorded and estimated parameters were recorded closer to the pin support. Higher values of average increment of these parameters were also found for this part. For the modulus of elasticity in bending, the increase was 11%.

Table 6. Average values of analysed parameters for ultimate limit state

Seria	$S1_{Fmax}$ [kN]	$S2_{Fmax}$ [kN]	F_{max} [kN]	u_{Fmax} [mm]	T_{Fmax} [s]	$M1_{Fmax}$ [kNm]	$M2_{Fmax}$ [kNm]	M_{avFmax} [kNm]	MOE [GPa]
A	17.54	20.36	37.91[1]	39.57	338.05	16.55[1]	17.56[1]	17.06	14.16[1]
F	24.84 (+42%)	27.57 (+35%)	52.41 (+38%)	54.57 (+38%)	430.52 (+27%)	23.09 (+40%)	24.07 (+37%)	23.58 (+38%)	15.71 (+11%)

[1] Values published in work [22]

3.2. The effect of testing conditions on the distribution of internal forces

The impact of the adopted load methodology on the distribution of internal forces and the recorded force values in individual actuators are discussed on the example of the F4 beam. The graphs (Figures 7 and 8) show areas of values for the A beams, plotted through the contours of all curves for individual elements.

The following graphs show the increasing variation in actuator values and estimated bending moment values in the final stages of the test. This phenomenon is most noticeable when the element is partially damaged during loading. The tests continued until the elements had been completely destroyed.

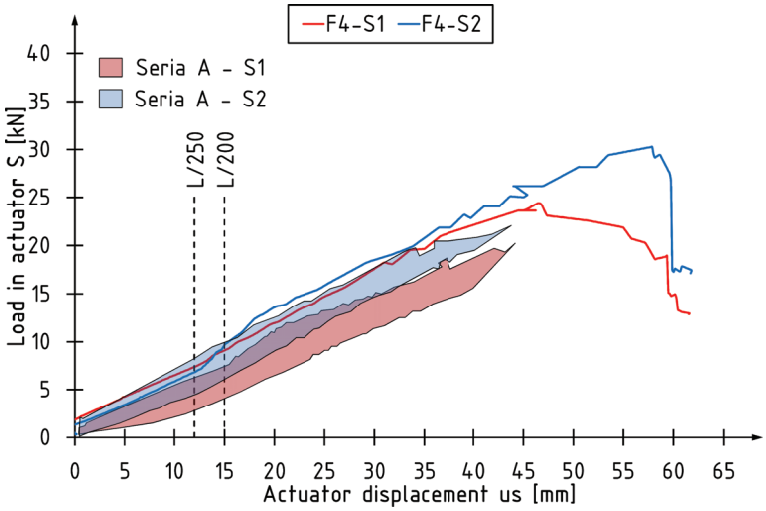

Fig. 7. The load in actuator – actuator displacement diagram for F4 beam

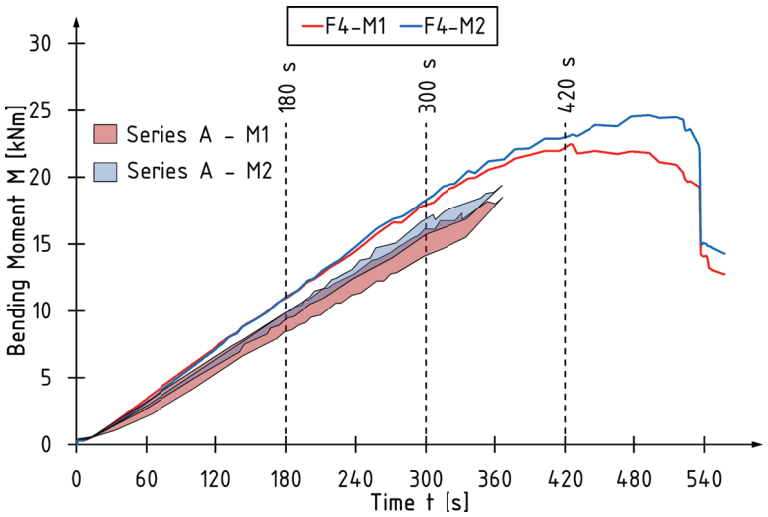

Fig. 8. The bending moment – time diagram for F4 beam

3.3. Failure mode

The reference beams were destroyed due to the exhaustion of strength in the extreme tensile fibres – in the middle of the beam. The destruction was brittle, sudden, and not indicated. Figure 9 shows the destruction of an element initiated in the place of local cross-section width reduction – a fragment removed from the outer veneer layer at a knot.

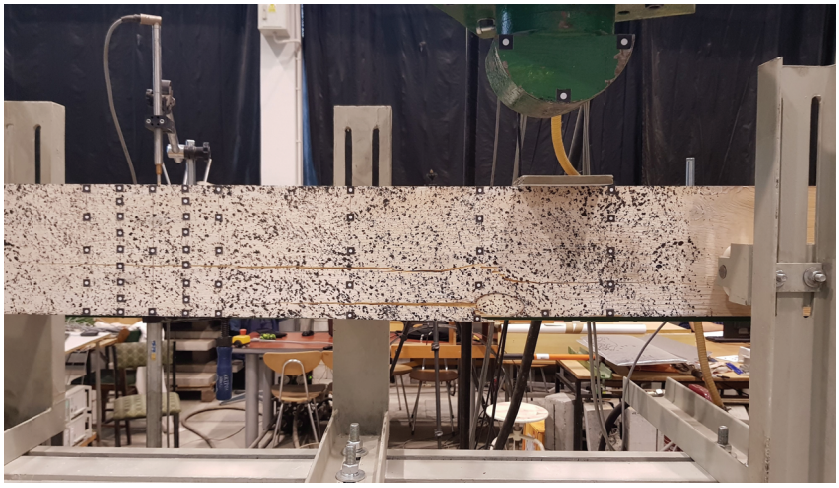

Fig. 9. Failure mode of unstrengthened beam – A1 (tension)

A typical failure mode of the reinforced beam resulted from exhaustion of the load bearing strength in the compressive zone (Fig. 10). The beginning of destruction was indicated by crackling or slow

crack propagation. In two cases, crack propagation caused the CFRP strip to debond combined with a crack in the tension zone. The CFRP strip was not ripped in any of the cases analysed.

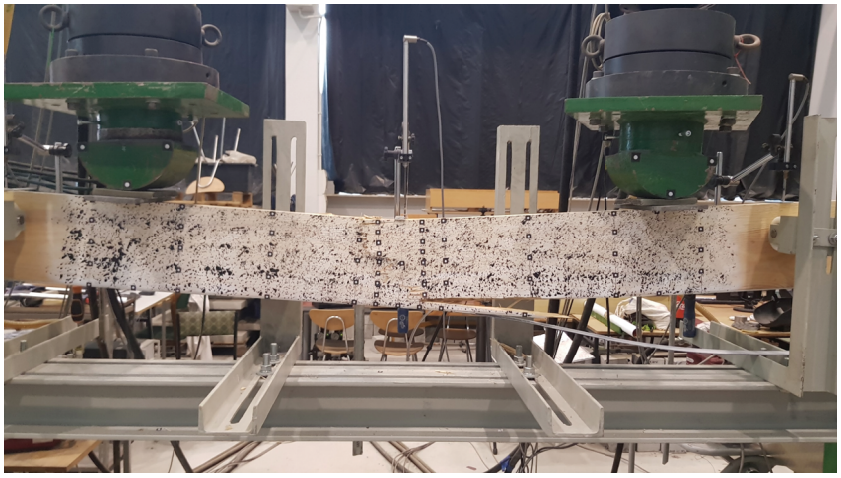

Fig. 10. Failure mode of strengthened beam – F1 (compression + tension + debonding)

3.4. Analytical analysis

The transformed cross-section method was used in order to evaluated the maximum stress in LVL and utilization of CFRP laminate. 14 GPa and 200 GPa values of modulus of elasticity for LVL and CFRP laminates were assumed respectively. Figure 11 shows the transformed cross section of F series beam.

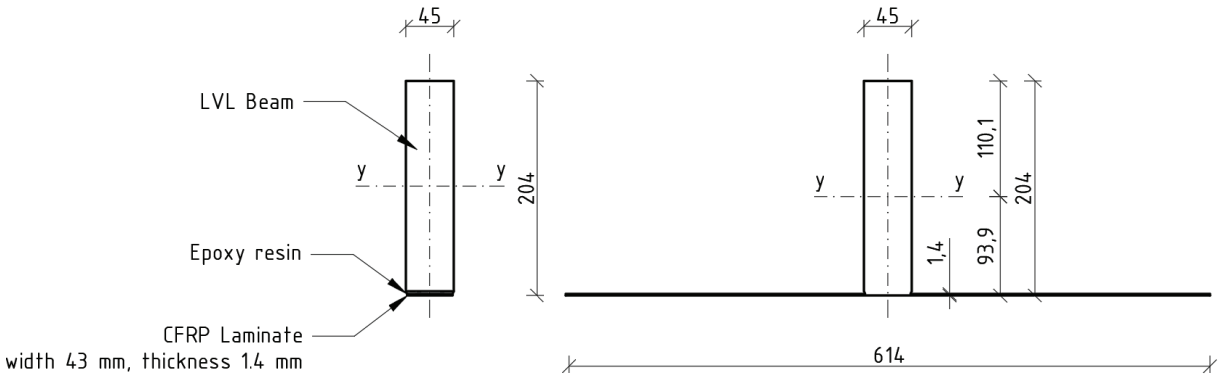

Fig. 11. Transformed cross section of F series beam

Average stress in CFRP laminate at destruction was 905MPa what is equal to 40% of its tensile strength. Maximum average stress at in LVL was 50.96 MPa.

4. Summary and conclusion

The paper presents the results of the experimental tests on reinforcement of laminated veneer lumber beams with CFRP strips glued to external surfaces. It was found:

1. The increase in load bearing capacity – maximum loading force and bending moment in the middle of the span of the reinforced beams – was 38%. The average global modulus of elasticity was increased by 11%.
2. Loading the beams by means of two actuators controlled by the loading speed of the actuators allows a more accurate presentation of the distribution of cross-sectional forces and the continuation of bending of elements in the event of partial failure of beam. The way the load was applied affected the differentiation of the force values in individual actuators in the final stage of the test.
3. The presented method of reinforcement may be applied to existing structures. The CFRP strips were glued between the support points of the elements, in the beam span.
4. The reference beams were destroyed due to the exhaustion of the load bearing capacity in the tensile zone. In the case of reinforced beams, the initiation of destruction took place in the compressive zone. Crack propagation in two cases caused the CFRP strip to debonding and a crack the tensile zone. The CFRP strip was not destroyed despite debonding.

Compared to the reinforcement glued into slots described in the paper [22], reinforcement by gluing the elements to the external surface requires less work both during the preparation of the reinforcement system components and the application of the reinforcement itself. The time of reinforcement application and aftertreatment is also shorter for the method presented in this paper. The F series is characterized by higher reinforcement effectiveness in terms of load bearing capacity of the elements, using reinforcement with a similar surface area to the E series. There were no significant differences in the global modulus of elasticity values.

Acknowledgement:

This article publication (Open Access and Article Processing Charge (APC)) was financed under the 02.0.12.00/2.01.01.00.0000, SUBB.BKWM.21.002 project.
The author would also like to thank S&P Polska Sp. z o.o. for the research materials provided.

References

[1] A. Borri, M. Corradi, "Strengthening of timber beams with high strength steel cords", *Composites: Part B*, vol. 42, no. 6, pp. 1480–1491, 2011. https://doi.org/10.1016/j.compositesb.2011.04.051

[2] A. Borri, M. Corradi, A. Grazini, "A method for flexural reinforcement of old wood beams with CFRP materials", *Composites: Part B*, vol. 36, no. 2, pp. 143–153, 2005. https://doi.org/10.1016/j.compositesb.2004.04.013

[3] A. D'Ambrisi, F. Focacci, R. Luciano, "Experimental investigation on flexural behavior of timber beams repaired with CFRP plates", *Composite Structures*, vol. 108, pp. 720–728, 2014. https://doi.org/10.1016/j.compstruct.2013.10.005

[4] A. De Jesus, J. Pinto, J. Morais, "Analysis of solid wood beams strengthened with CFRP laminates of distinct lengths", *Construction and Building Materials*, vol. 35, pp. 817–828, 2012. https://doi.org/10.1016/j.conbuildmat.2012.04.124

[5] B. Anshari, Z.W. Guan, A. Kitamori, K. Jung, K. Komatsu, "Structural behaviour of glued laminated timber beams pre-stressed by compressed wood", *Construction and Building Materials*, vol. 29, pp. 24–32, 2012. https://doi.org/10.1016/j.conbuildmat.2011.10.002

[6] E.R. Thorhallsson, G.I. Hinriksson, J.T. Snæbj€ornsson, "Strength and stiffness of glulam beams reinforced with glass and basalt fibres", *Composites: Part B*, vol. 115, pp. 300–307, 2016. https://doi.org/10.1016/j.compositesb.2016.09.074

[7] F.H. Theakston, "A feasibility study for strengthening timber beams with fiberglass", *Canadian agricultural engineering*, 1965, pp. 17-19.

[8] G.M. Raftery, A.M. Harte, "Low-grade glued laminated timber reinforced with FRP plate", *Composites: Part B*, vol. 42, no. 4, pp. 724–735, 2011. https://doi.org/10.1016/j.compositesb.2011.01.029

[9] G.M. Raftery, F. Kelly, "Basalt FRP rods for reinforcement and repair of timber", *Composites: Part B*, vol. 70, pp. 9–19, 2015. https://doi.org/10.1016/j.compositesb.2014.10.036

[10] H. Gezer, B. Aydemir, "The effect of the wrapped carbon fiber reinforced polymer material on fir and pine woods", *Materials and Design*, vol. 31, no. 7, pp. 3564–3567, 2010. https://doi.org/10.1016/j.matdes.2010.02.031

[11] H. Yang, D. Ju, W. Liu, W. Lu, "Prestressed glulam beams reinforced with CFRP bars", *Construction and Building Materials*, vol. 109, pp. 73–83, 2016. https://doi.org/10.1016/j.conbuildmat.2016.02.008

[12] H. Yang, W. Liu, W. Lu, S. Zhu, Q. Geng, "Flexural behavior of FRP and steel reinforced glulam beams, Experimental and theoretical evaluation", *Construction and Building Materials*, vol. 106, pp. 550–563, 2016. https://doi.org/10.1016/j.conbuildmat.2015.12.135

[13] I. Glišović, B. Stevanović, M. Todorović, T. Stevanović, "Glulam beams externally reinforced with CFRP plates", *Wood research*, vol. 61, no. 1, pp. 141–154, 2016.

[14] J.A. Balmori, L.A. Basterra, L. Acuña, "Internal GFRP Reinforcement of Low-Grade Maritime Pine Duo Timber Beams", *Materials*, vol. 13, no. 3, 571, 2020. https://doi.org/10.3390/ma13030571

[15] J. Soriano, B.P. Pellis, N.T. Mascia, "Mechanical performance of glued-laminated timber beams symmetrically reinforced with steel bars", *Composite Structures*, vol. 150, pp. 200–207, 2016. https://doi.org/10.1016/j.compstruct.2016.05.016

[16] K. Andor, A. Lengyel, R. Polgár, T. Fodor, Z. Karácsonyi, "Experimental and statistical analysis of spruce timber beams reinforced with CFRP fabric", *Construction and Building Materials*, vol. 99, pp. 200–207, 2015. https://doi.org/10.1016/j.conbuildmat.2015.09.026

[17] L.A. Basterra, J.A. Balmori, L. Morillas, L. Acuña, M. Casado, "Internal reinforcement of laminated duo beams of low-grade timber with GFRP sheets", *Construction and Building Materials*, vol. 154, pp. 914–920, 2017. https://doi.org/10.1016/j.conbuildmat.2017.08.007

[18] L. Rudziński, "Konstrukcje drewniane. Naprawy, wzmocnienia, przykłady obliczeń", Skrypt Politechniki Świętokrzyskiej, Kielce, 2010.

[19] L. Ye, B. Wang, P. Shao, "Experimental and Numerical Analysis of a Reinforced Wood Lap Joint", *Materials*, vol. 13, no. 18, 4117, 2020. https://doi.org/10.3390/ma13184117

[20] M. Bakalarz, P. Kossakowski, "Mechanical Properties of Laminated Veneer Lumber Beams Strengthened with CFRP Sheets", *Archives of Civil Engineering*, vol. 65, no. 2, pp. 57–66, 2019. https://doi.org/10.2478/ace-2019-0018

[21] M. Bakalarz, P. Kossakowski, "The flexural capacity of laminated veneer lumber beams strengthened with AFRP and GFRP sheets", *Technical Transactions*, vol. 2, pp. 85–95, 2019. https://doi.org/10.4467/2353737XCT.19.023.10159

[22] M.M. Bakalarz, P.G. Kossakowski, P. Tworzewski, "Strengthening of Bent LVL Beams with Near-Surface Mounted (NSM) FRP Reinforcement", *Materials*, vol. 13, no. 10, pp. 1–12, 2020. https://doi.org/10.3390/ma13102350

[23] M. Corradi, A. Borri, "Fir and chestnut timber beams reinforced with GFRP pultruded elements", *Composites: Part B*, vol. 38, no. 2, pp. 172–181, 2007. https://doi.org/10.1016/j.compositesb.2006.07.003

[24] M. Dudziak, I. Malujda, K. Talaśka, T. Łodygowski, W. Sumelka, "Analysis of the process of wood plasticization by hot rolling", *Journal of Theoretical and Applied Mechanics*, vol. 54, no. 2, pp. 503–516, 2016. https://doi.org/10.15632/jtam-pl.54.2.503
[25] M. Fossetti, G. Minafò, M. Papia, "Flexural behaviour of glulam timber beams reinforced with FRP cords", *Construction and Building Materials*, vol. 95, pp. 54-64, 2015. https://doi.org/10.1016/j.conbuildmat.2015.07.116
[26] P. De La Rosa, A. Cobo, M.N. González García, "Bending reinforcement of timber beams with composite carbon fiber and basalt fiber materials", *Composites: Part B*, vol. 55, pp. 528–536, 2013. https://doi.org/10.1016/j.compositesb.2013.07.016
[27] P. De La Rosa García, A.C. Escamilla, M.N. González García, "Analysis of the flexural stiffness of timber beams reinforced with carbon and basalt composite materials", *Composites: Part B*, vol. 86, pp. 152–159, 2016. https://doi.org/10.1016/j.compositesb.2015.10.003
[28] P.G. Kossakowski, "Influence of anisotropy on the energy release rate GI for highly orthotropic materials", *Journal of Theoretical and Applied Mechanics*, vol. 45, no. 4, pp. 739–752, 2007.
[29] PN-EN 14374:2005 Timber Structures. Structural Laminated Veneer Lumber (LVL). Requirements, Polish Standards Committee: Warsaw, Poland, 2005.
[30] PN-EN 1995-1-1:2010 Eurocode 5, Design of timber structures. Part 1-1: General. Common rules and rules for buildings, Polish Standards Committee: Warsaw, Poland, 2010.
[31] PN-EN 408+A1:2012 Timber Structures. Structural Timber and Glued Laminated Timber. Determination of Some Physical and Mechanical Properties, Polish Standards Committee: Warsaw, Poland, 2012.
[32] PN-EN 527-1:2012 Plastics. Determination of tensile properties. Part 1: General principles, Polish Standards Committee: Warsaw, Poland, 2013.
[33] PN-EN 527-5:2010 Plastics. Determination of tensile properties. Part 5: Test conditions for unidirectional fibre-reinforced plastic composites, Polish Standards Committee: Warsaw, Poland, 2010.
[34] T.P. Nowak, J. Jasieńko, D. Czepiżak, "Experimental tests and numerical analysis of historic bent timber elements reinforced with CFRP strips", *Construction and Building Materials*, vol. 40, pp. 197–206, 2013. https://doi.org/10.1016/j.conbuildmat.2012.09.106
[35] V. De Luca, C. Marano, "Prestressed glulam timbers reinforced with steel bars", *Construction and Building Materials*, vol. 30, pp. 206–217, 2012. https://doi.org/10.1016/j.conbuildmat.2011.11.016
[36] Y. Nadir, P. Nagarajan, M. Ameen, M. Arif M, "Flexural stiffness and strength enhancement of horizontally glued laminated wood beams with GFRP and CFRP composite sheets", *Construction and Building Materials*, vol. 112, pp. 547–555, 2016. https://doi.org/10.1016/j.conbuildmat.2016.02.133
[37] Y.-F. Li, M.-J. Tsai, T.-F. Wei, W.-C. Wang, "A study on wood beams strengthened by FRP composite materials", Construction and Building Materials, vol. 62, pp. 118–125, 2014. https://doi.org/10.1016/j.conbuildmat.2014.03.036
[38] Y.-F. Li, Y.-M. Xie, M.-J. Tsai, "Enhancement of the flexural performance of retrofitted wood beams using CFRP composite sheets", *Construction and Building Materials*, vol. 23, pp. 411–422, 2009. https://doi.org/10.1016/j.conbuildmat.2007.11.005
[39] Z.W. Guan, P.D. Rodd, D.J. Pope, "Study of glulam beams pre-stressed with pultruded GRP", *Computers and Structures*, vol. 83, pp. 2476–2487, 2005. https://doi.org/10.1016/j.compstruc.2005.03.021

Nośność na zginanie belek z forniru klejonego warstwowo wzmocnionych taśmami CFRP

Słowa kluczowe: 4-punktowe zginanie, konstrukcje drewniane, włókna węglowe, zbrojenie

Streszczenie:

W pracy przedstawiono wyniki badań eksperymentalnych dotyczących wzmacniania zginanych belek z forniru klejonego warstwowo za pomocą taśm węglowych (CFRP) przyklejanych do powierzchni dolnej elementów. Taśmy CFRP, o wymiarach 1,4×43×2800 mm, przyklejone zostały za pomocą żywicy epoksydowej. Badania przeprowadzono na elementach pełnowymiarowych o wymiarach nominalnych 45×200×3400 mm. Belki obciążano symetrycznie dwoma siłami skupionymi do zniszczenia. Na podstawie wyników badań stwierdzono:

1. Wzrost nośności – maksymalnej siły obciążającej oraz momentu zginającego w środku rozpiętości – belek wzmocnionych wyniósł 38%. Przyrost przeciętnej wartości modułu sprężystości wyniósł 11%.

2. Obciążanie belek za pomocą dwóch siłowników kontrolowanych za pomocą prędkości ich przesuwu umożliwia dokładniejsze przedstawienie rozkładu sił wewnętrznych w przekroju całego badania oraz kontynuacje zginania w przypadku wystąpienia częściowego zniszczenia w obrębie jednego z siłowników. Sposób prowadzenia obciążenia wpłynął na zróżnicowanie wartości sił w poszczególnych siłownikach w końcowej fazie badania.
3. Przedstawiony sposób wzmocnienia może zostać zastosowany w przypadku konstrukcji istniejących. Taśmy przyklejone zostały pomiędzy punktami podparcia elementów w części przęsłowej belki.
4. Belki referencyjne ulegały zniszczeniu na skutek wyczerpania nośności w strefie rozciąganej. W przypadku belek wzmocnionych inicjacja zniszczenia następowała w strefie ściskanej. Propagacja pęknięcia w dwóch przypadkach wywołała odspojenie taśmy CFRP oraz pękniecie w strefie rozciąganej. Taśmy CFRP pomimo odspojenia nie ulegały zniszczeniu.

Received: 2020-11-17, Revised: 2021-02-03